Scientific Research Publishing

International Journal of Geosciences, 2022, 13, 464-482
https://www.scirp.org/journal/ijg
ISSN Online: 2156-8367
ISSN Print: 2156-8359

The Influence of an Interdependent Structures on the Post-Mesozoic Evolution of the Eastern Flank of the Mongol-Okhotsk Orogenic Belt

Inna Derbeko

Institute of Geology and Nature Management, Far Eastern Branch Russian Academy of Sciences, Blagoveschensk, Russia
Email: derbeko@mail.ru

How to cite this paper: Derbeko, I. (2022) The Influence of an Interdependent Structures on the Post-Mesozoic Evolution of the Eastern Flank of the Mongol-Okhotsk Orogenic Belt. *International Journal of Geosciences*, **13**, 464-482.
https://doi.org/10.4236/ijg.2022.136025

Received: February 18, 2022
Accepted: June 21, 2022
Published: June 24, 2022

Abstract

Based on the analysis of known geodynamic models that explain the processes in various geodynamic settings of the Meso-Cenozoic stages of the development of continental margins and the tectonic-magmatic events accompanying these processes, as well as on the basis of our own data obtained as a result of many years of research on the axial structure of the Central Asian Fold Belt-Mongol-Okhotsk orogenic belt and the influence of interdependent structures on the post-Mesozoic evolution of the eastern flank of the Mongol-Okhotsk orogenic belt was substantiated by us. The closure of the Mongol-Okhotsk basin due to the approach of the Siberian and North China cratons was accompanied by a change in geodynamic conditions: subduction, collision, intraplate-rift and was reflected in the formation of synchronous igneous complexes in the frame of the Mongol-Okhotsk orogenic belt. In the northern frame of the belt, the distribution of magmatites is cut off by the structure of the Selenga-Stanovoy superterrane in the west. The northern boundary of the superterrane is the zone of the Dzheltulak fault. In the south, it borders on the Mongol-Okhotsk orogenic belt along the zone of tectonic melange. We believe that evolutionary processes within the orogenic belt and its framing continued into the post-Mesozoic time after the final formation of the belt as an orogen. The position of the Selenga-Stanovoy superterrane in the late Mesozoic did not correspond to the modern one. The structures of the Central Asian fold belt located between the Mongol-Okhotsk orogenic belt and the Siberian craton in the Cenozoic were influenced by collisional processes occurring between the Indian and Eurasian plates. And these processes were not only the "driving force" for the movement of the Selenga-Stanovoy superterrane in the post-Mesozoic time, but also changed the structure of the Mongol-Okhotsk orogen, dividing it into two flanks.

Keywords

Mongol-Okhotsk Orogenic Belt, Magmatism, Late Mesozoic, Subduction, Collision, Tectonic Events

1. Introduction

The Mongol-Okhotsk Orogenic Belt (MOOB) is recognized as the axial structure of the Central Asian Folded Belt (CAFB) [1]. The final formation of the MOOB in the Late Mesozoic is the final completion of the formation of CAFP as an orogen. But the tectonic, geodynamic and magmatic processes that took place in the post-Mesozoic influenced the evolution of these regional structures. MOOB stretched from Inner Mongolia to the Pacific coast for 3000 km. Its formation is associated with the convergence of the Siberian and North China cratons and the closure of the Mongol-Okhotsk basin in the Late Mesozoic. Post-Mesozoic tectonic events have changed its original appearance. In the region of the 120th meridian, two cratons approached each other as close as possible, "absorbing" the formations of the belt itself, and divided it into the western and eastern flanks (**Figure 1(a)**).

The article considers the eastern flank of the belt. In the frame of this flank, from the end of the Jurassic to the beginning of the Late Cretaceous, the magmatic complexes of various compositions were formed almost continuously. Long-term studies of this territory have not led to an unambiguous view of the evolution of the region. The precise geochronological, isotopic, geochemical, and geophysical data obtained in recent years allow us to take a fresh look at the development of this complex region.

The solution to this problem was based on the study of magmatites in the frame of the MOOB. The material characteristics of rocks reflect not only their composition but also the geodynamic conditions that they accompany during their formation.

2. Materials and Methods

To establish what geological events influenced the post-Mesozoic evolution of the MOOB, not only the original data of the author were analyzed, but also the results of recent geochronological, isotopic, geochemical studies of magmatic complexes accompanying the evolution of the MOOB in the late Mesozoic-Cenozoic were analyzed (eg, [4]-[11]). The results of geophysical research are also used-transects passing through the MOOB [12] [13] [14] [15].

2.1. Petrological and Geochemical Studies

The current research presents the results of petrological and geochemical studies, which were carried out according to the following methods. The content of petrogenic elements (main petrogenic components Sr, Zr, Nb) in the samples

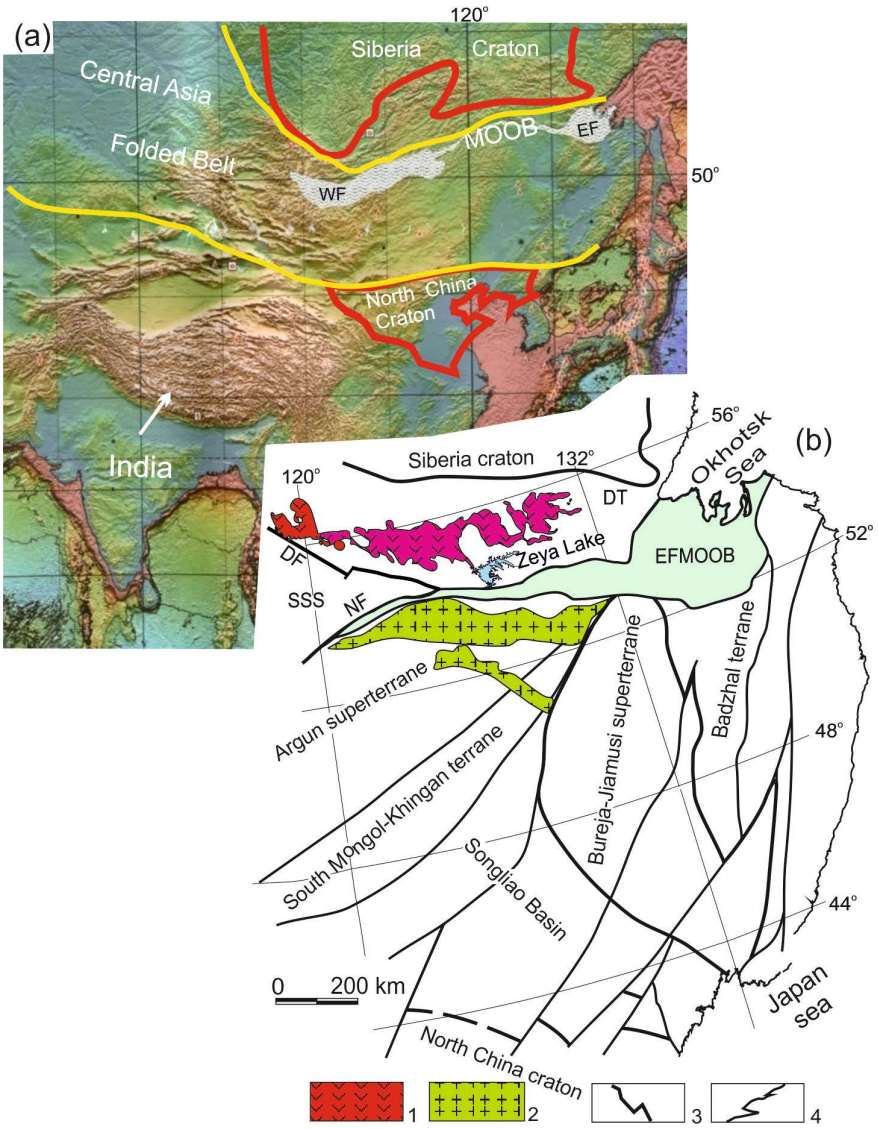

Figure 1. The location of the MOOB among the main structures of the region. (a) The location of the MOOB among the main structures of the region based "Geological map of the World", scale 1:50,000,000 (after [2]). Letter abbreviations: MOOB—Mongol-Okhotsk orogenic belt, WF—West and EF—East flank of belt. The arrow indicates the direction of movement of the Indian plate in the Cenozoic. (b) The scheme tectonic zoning of the east flank of the MOOB [1] [3] and the location of magmatic formations in its frame. Area of distribution of Late Mesozoic magmatic complexes: mainly plutonic (1), mainly volcanogenic (2), Structural tectonic faults (3), other faults (4). Letter abbreviations: EMOOB—East flank of Mongol-Okhotsk orogenic belt SSS—Selenga-Stanovoy superterrane, BT—Badzal terrane, DF—Dzheltulak fault, NF—North-Tukuringra fault.

was determined by X-ray fluorescence (XFR) analysis using the S4 PIONEER spectrometer in the Institute of Geology and Nature Management, Far East Branch of the Russian Academy of Sciences (Blagoveshchensk, Russia). Analysis of the rare-earth elements (Ga, Ge, Rb, Cs, Sr, Ba, Pb, La, Ce, Pr, Nd, Sm, Eu, Gd, Tb, Dy, Ho, Er, Tm, Yb, Lu, Y, Th, U, Zr, Hf, Nb, Ta, Sc) was made inductively coupled mass spectrometry (ICP-MS) in the Institute of Analytical In-

strumentation of the Russian Academy of Sciences (Saint Petersburg, Russia).

To perform the XFR analysis, the powder sample was homogenized by fusion with lithium metaborate (flux) in a muffle furnace at 1150˚C. The measurements were carried out using Pioneer 4S X-ray spectrometer (Bruker, Germany). The intensity values of analytical lines were adjusted against the background, absorption and secondary fluorescence. For the ICP-MS analysis, the samples were extracted by acid decomposition. The measurements were carried out on the "PlasmaQuad" by the "VG Elemental" company, in standard mode. The sensitivity calibration over the entire mass scale was performed using a multi-element standard solution of rare-earth elements produced by "Matthew Johnson". The relative error of measurements was 3% - 10%.

2.2. Isotope-Geochemical Studies

Isotope-geochemical studies were carried out at the Institute of Geology of Ore Deposits, Petrography, Mineralogy, and Geochemistry of the Russian Academy of Sciences (Moscow) under the supervision of A.V. Chugaev.

The contents of Rb, Sr, Sm, and Nd and the isotope ratios of $^{87}Rb/^{86}Sr$ and $^{147}Sm/^{144}Nd$ in the rock samples were determined by isotopic dilution using mixed ^{85}Rb-^{84}Sr and ^{149}Sm-^{150}Nd tracers, which were added to the samples immediately before their chemical decomposition. The decomposition of gross rock samples, the sample weight of which varied from 0.1 to 0.2 g, was carried out in a mixture of concentrated acids HF + HNO_3 (3:1). Samples were kept in a sealed autoclave at a temperature of about 160˚C until completely dissolved.

Rb, Sr, Sm, and Nd preparations for mass spectrometric analysis were obtained using the method of two-stage ion-exchange chromatography. At the first stage, the fractions of Rb, Sr, and light REE were separated from the elements of the sample matrix. The fractions were isolated in 2.4 M HCl on ion-exchange columns filled with 3 ml of BioRad W50x8 cation exchanger (200 - 400 mesh). Chromatographic separation of Nd and Sm from other REE lungs was carried out in the second stage, using columns filled with 0.5 ml of HDEHP ion-exchange resin deposited on Kel-F granules. The total level of background contamination of the sample during the entire procedure of chemical preparation for Sr and Nd did not exceed 0.1 ng.

Mass spectrometric measurements of the isotopic composition of Rb, Sr, Sm, and Nd were carried out on a multi-collector thermal ionization mass spectrometer Sector 54 (Micromass, United Kingdom). Correctness of measurements of isotope ratios $^{87}Sr/^{86}Sr$ and $^{143}Nd/^{144}Nd$ was controlled by systematic measurements of the international standard for Sr isotopic composition (SRM-987) and the intralaboratory sample of the Nd "Nd-IGEM" isotopic composition calibrated against the international LaJolla standard. The error in the measured ratios $^{87}Sr/^{86}Sr$ and $^{143}Nd/^{144}Nd$ did not exceed 0.003% ($\pm 2\sigma$ed). The accuracy of determination of the $^{87}Rb/^{86}Sr$ and $^{147}Sm/^{144}Nd$ isotopic ratios was 0.5% and 0.2%, respectively ($\pm 2\sigma$ units).

3. Results

As a result of studies [3] [7] [8] [9] [10] [16] [17], it was found that in the southern and northern framing of the eastern flank of the MOOB, volcano-plutonic and volcanogenic complexes were formed starting from the turn of the Late Jurassic and Early Cretaceous. They were accompanied by various geodynamic settings. The belonging of these complexes to certain structures was revealed. In the northern frame of the belt, the Selenga-Stanovoy (SSS) and Dzhugdzhur-Stanovoy (DSS) are distinguished—the southern frame of the Siberian craton—superterranes. The southern boundary of the belt is represented by the Argun and Bureya-Jiamusi superterranes and the South Mongolian–Khingan orogenic belt (**Figure 1(b)**). It has been established that within the southern framing of the Siberian craton, the Argun superterrane, and the South Mongol-Khingan orogenic belt, rocks of homogeneous composition and formation time were formed. Their formation took place at the following magmatic stages.

Stage I: Magmatism within the listed structures first appeared 145 - 138 Ma ago. During this period, adakite volcanoplutonic complexes begin to form [10] [16] [17]. The rocks of these complexes are not widespread. They are represented by subalkaline granites, leucogranites, granites, subalkaline leucogranites, granosyenites and their porphyry varieties. These are rocks of the normal or subalkaline series, high potassium, belong to the calc-alkaline series, with $Na_2O + K_2O$ = 7.86 - 10.92 wt% and Na_2O/K_2O = 1.25 - 1.81. The rocks are magnesian and peraluminous at ASI (aluminum saturation index) = 1.06 - 0.86, which characterizes them as I-type formations [18] (Zen, 1986). Elevated concentrations of Sr (670 - 1110 ppm), Ba (510 - 2400 ppm) were found in the rocks; Rb (82 - 160 ppm), Th (8.4 - 13.1 ppm); at low contents of Nb (4.0 - 11.0 ppm), Ta (0.4 - 0.6 ppm) and at abnormally low concentrations of HREE (in ppm): Tb (0.18 - 0.22), Dy (0.66 - 1.45), Ho (0.10 - 0.22); Er (0.25 - 0.55); Tm (0.03 - 0.07); Lu (0.02 - 0.05), as well as Y (3 - 7) and Yb (0.17 - 0.42). Chondritic-normalized diagrams show a positive Eu anomaly or its absence: (Eu/Eu*)n = 0.77 - 1.23 at (La/Yb) n = 26.45 - 64.13 (**Figure 2**).

On the classification diagrams (La/Yb)n-Ybn [20] [21] and Sr/Y-Y [22], the figurative points of this complex rocks are projected onto the rock field of typical adakite series of the world. According to the isotope-geochemical characteristics, they belong to the negative εNd-type with εNd(T) = (−3.3) - (−4.6). The values of $^{87}Sr/^{86}Sr$ are 0.7069 - 0.7071.

By its formation time (145 - 138 Ma), the adakite series rocks preceded (and partly coincided) the formation of the Early Cretaceous calc-alkaline complex: 140 - 128 Ma.

The formation of the adakite complex rocks was replaced by the formation of the rocks of a differentiated granite-granodiorite complex (140 - 128 Ma) [4] [17] [23] [24] [25]. These granitoids compose both large batholiths with an area of up to 500 km^2, and small bodies of the complex and dyke-shaped forms (**Figure 1(b)**). They are widely spread in the northern frame of the belt. This can be

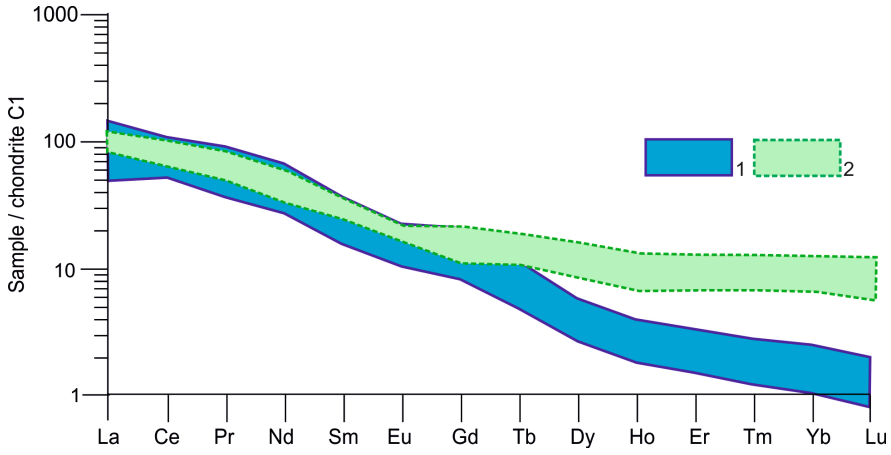

Figure 2. Trace element concentrations normalized to the composition of chondrite C_1 according to [19] in the rocks of the northern and southern frames of the MOOB (1 - 2): adakite series (145 - 138 Ma)—1; for comparison, integrated data of rocks are given calc-alkaline series (140 - 122 Ma)—2.

explained by the strong erosion of this part of the region. The complex contains granodiorites, quartz diorites, granites, plagiogranites, and leucogranites.

According to the SiO_2 content, granitoids belong to the formations of the calc-alkaline series with a ratio of Na_2O/K_2O = 0.9 - 1.6. The amount of alkali is almost constant for all varieties (6.1 - 7.1 wt%) With a content of K_2O = 2.3 - 3.3, and Na_2O = 3.1 - 4.1 wt%. These are mainly high-potassium rocks of the peraluminous series at ASI = 0.9 - 1.2. They are characterized by moderate to low titanium. The strontium isotopic ratios of the granitoids of the complex are: $^{87}Sr/^{86}Sr$ = 0.7076 - 0.7068 [25].

The formation of hypabyssal granitoids of monzodiorite-granodiorite composition is shifted in time of formation: 130 - 126 Ma [4] [23] [24] [25]. They form large area laccoliths and lopoliths (up to 200 km^2) composed of porphyritic quartz diorites, monzonites, quartz monzonites, granodiorites. The rocks of the complex belong to the high potassium calc-alkaline series at Na_2O/K_2O = 0.9 - 2.2. They are characterized by an almost constant content of Al_2O_3 (15.1 - 16.1 wt%) at ASI = 1.1 - 1.3, belong to the potassium-sodium series, moderately magnesian, moderately titanic.

Granitoids with an age of 130 - 126 Ma are comagmatic of a volcanic complex with an age of 128 - 122 Ma. The rocks of this complex are composed of paleo volcanoes of the central type. They are represented by andesite basalts, andesites, trachyandesites, dacite andesites, dacites, their tuffs, tuff aleurolites, tuff sandstones. According to the petrochemical features, volcanic are the rocks with a predominantly sodium type of alkalinity: Na_2O/K_2O = 0.81 - 2.66, with a total of alkalis from 4.6 to 6.9 wt%. Volcanites from low to high potassium species, moderately to low titanium; moderate to high magnesian, are belonging to the calc-alkaline series. Alumina varies from moderate to high (ASI = 1.0 - 1.3).

For andesites of the volcanic complex, the ratios $^{87}Sr/^{86}Sr$ = 0.7063 - 0.7078 were established [24], which are comparable to earlier plutonic formations.

According to the REE content, all formations of the beginning of the Early Cretaceous are comparable among themselves, which is reflected in the diagrams (**Figure 3(a)**).

Their compositions on chondritic-normalized plots are characterized by a hollow oblique shape, with an almost absent Europium anomaly (Eu/Eu* = 0.7 - 0.91).

It can be stated that in the range of 140 - 122 Ma differentiated calc-alkaline volcano plutonic complexes are formed with common geochemical characteristics that indicate the unity of the geodynamic conditions of their formation. These conditions (**Figure 3(b)**) correspond to suprasubduction environments of the active continental margins of the Andean type [16] [17].

Stage II: The development fields of bimodal volcano-plutonic complexes (**Figure 1(b)**) are territorially combined with the distribution fields of differentiated plutonic and volcanic formations of the calcareous-alkaline series of the beginning of the Early Cretaceous [7] [8]. Their formation began almost immediately after the completion of the formation of differentiated complexes and lasted

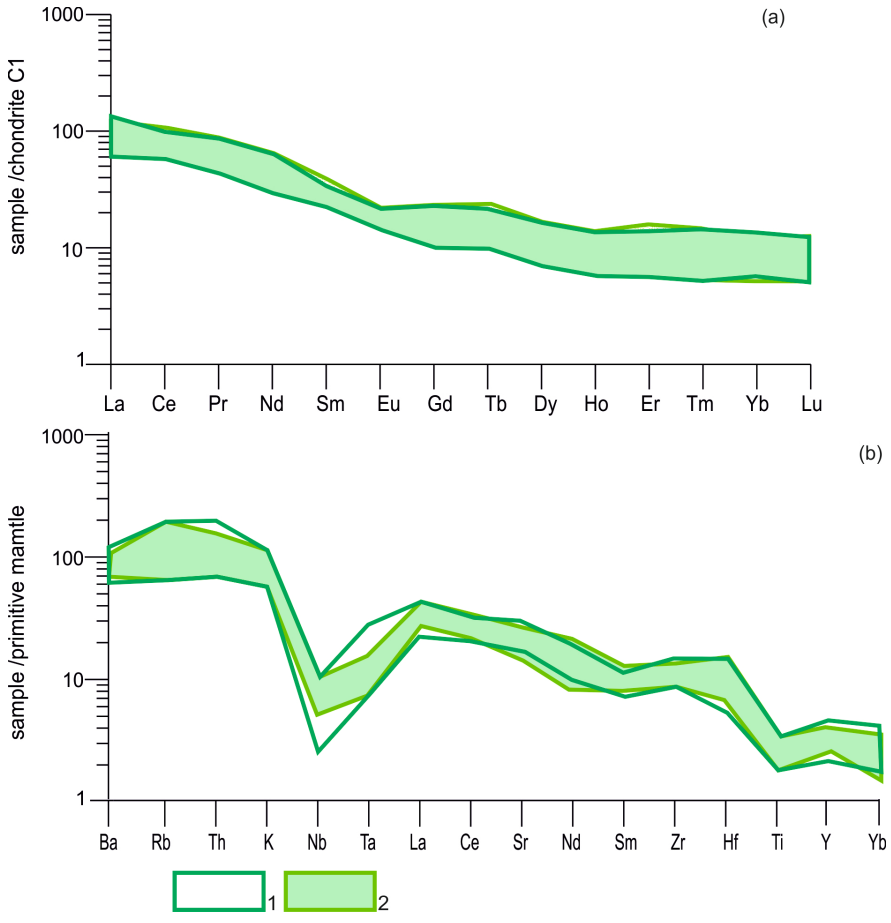

Figure 3. Concentrations of the rare elements of the rock calc-alkaline series (140 - 122 Ma) standardized to the composition of Chondrite (a) and primitive mantel (b). Compositions of chondrite C_1 and primitive mantel are brought according to the data [19]. Northern frames EFMOOB (1) and Southern frames EFMOOB (2).

more than 20 Ma: 119 - 97 Ma [7] [24] [25]. The formation of bimodal complexes accompanied the final formation of the MOOB [8] as an orogen.

Paleo volcanic structures composed with the rocks of bimodal complexes form more than 30 volcanic fields in both the northern and southern frames of the MOOB with an area of up to 200 km^2. In the structure of these fields the cover, vent and subvolcanic facies are distinguished. The percentage of rocks of the complex from its total volume is: the main composition—55%, the average—9%, sour—20%, tuff-sedimentary—16%.

The lavas of the primary-middle composition are represented by trachybasalts, trachyandesitic basalts, trachyandesites and andesites. The increased alkalinity of the lavas of basic to medium composition is due to the presence of potassium feldspar or red-brown biotite in the matrix of rocks, less commonly, sanidine in phenocrysts.

Acidic varieties are represented by rhyolites, rhyodacites, trachyriolites, with interbeds of perlites, tuffs and ignimbrites. The plutonic formations comagmatic to volcanic rocks correspond with subalkaline granites, subalkaline leucogranites, granodiorites, quartz diorites, and quartz monzonites. The bimodal composition of the rocks of the complex is due to two ranges of content SiO_2: 47 - 64 and 72 - 78 wt% at the absence of intermediate varieties. Volcanics with a SiO^2 content of 47 - 64 wt% are high alumina (Al_2O_3 = 15.22 - 17.30 wt%), moderately low magnesian, low titanium (TiO_2 < 2 wt%) formations. They belong mainly to the high potassium calc-alkaline series. Volcanics with a SiO_2 content of 72 - 78 wt% are characterized by normal, less often moderate alkalinity, with an increase in SiO_2 content, the total alkalinity decreases (from 9.13 to 7.13 wt%), low alumina content (Al_2O_3 = 11.15 - 13.96 wt%), low magnesian, low titanium They belong to the high potassium calc-alkaline series. Plutonic acidic formations belong to A-type granites, while granitoids comagmatic with medium-basic volcanics are comparable to I- and S-type formations [7].

All rocks of the bimodal complexes are enriched with light rare-earth elements (La/Yb)n = 5.5 - 33.0 (values of 10 - 20 prevail).

The Eu-minimum (**Figure 4(a)**) in basic-medium rocks is weakly expressed (Eu/Eu^* = 0.70 - 0.86), and in acid formations it is deeper (Eu/Eu^* = 0.33 - 0.70). The multielement spectra are characterized by stable negative anomalies of Nb (0.10 - 0.43), Ta (0.12 - 0.79) and Ti (0.01 - 0.09) for all rock varieties and a highly variable Sr anomaly: for granitoids and acidic volcanic rocks, it is negative, and for main-medium rocks - from weakly manifested negative to positive. Positive values indicate the contents of Ba, Rb, Th, K (**Figure 4(b)**).

The rocks of the bimodal complexes are characterized by sustained isotopic compositions with variations in the $^{87}Sr/^{86}Sr$ ratio (0.7057 - 0.7063, 0.7081 - 0.7084) and a wider range of $\varepsilon Nd(T)$ = (−0.6) - (−3.6) [24] [25] and authors data. Model Nd age - T_{Nd} (DM-2st) - is characterized by a relatively narrow interval of 975 - 1314 Ma, which may indicate the material uniformity of the melting substrate with the crustal component of the late Riphean. They are superimposed on

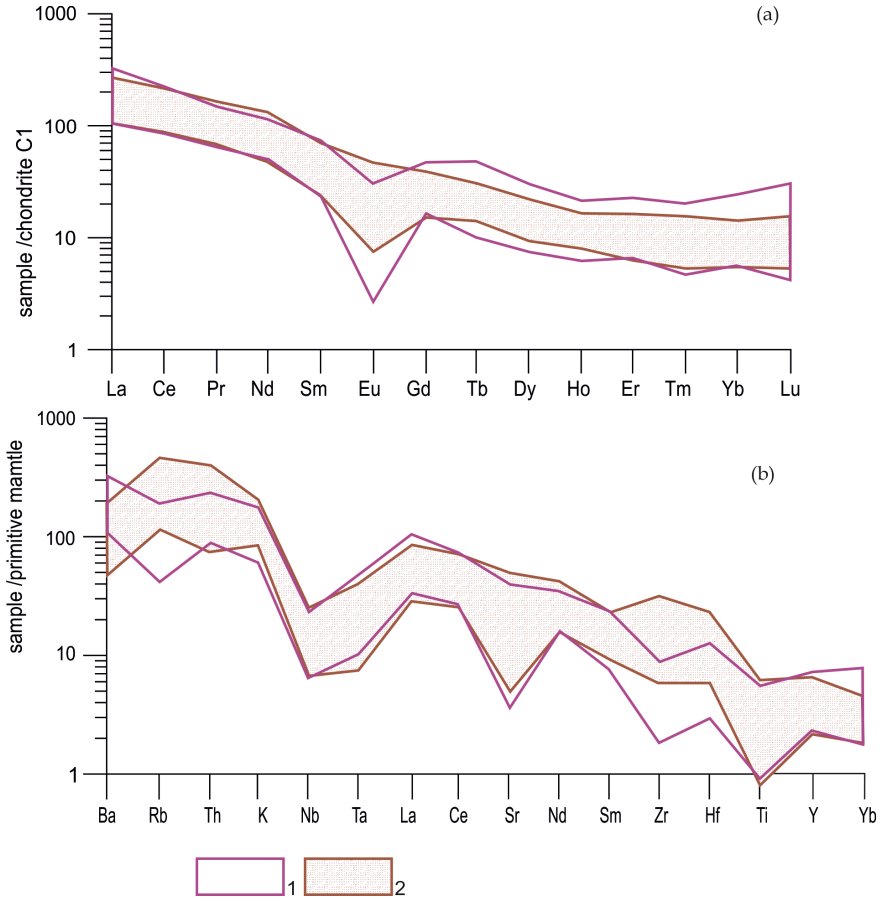

Figure 4. Concentrations of the rare elements of the rock bimodal series (119 - 97 Ma) standardized to the composition of Chondrite (a) and primitive mantel (b). Compositions of chondrite C_1 and primitive mantel are brought according to the data [19]. Northern frames EFMOOB (1) and Southern frames EFMOOB (2).

the northern edge of the Argun terrane and the southern border of the Siberian craton, where Precambrian formations are widely developed.

Summarizing the available geochronological dating of the isotope dating of the rock, carried out by the U-Pb method on zircons [24]; ^{40}Ar-^{39}Ar method [4] [7] [24] [25], we obtained the following time sequence of complex formation. Andesitic trachybasalts were formed from the lower part of the section—118.7 ± 0.9 million years; rhyolites, trachirhyolites—118.7; 118.4; 117 ± 1; 117.1; 117.6; 115.3 ± 1.5 Ma and trachyandesites—115 Ma, 114.7 ± 0.6 Ma (middle section). The upper part of the section is 105.9; 100; 97 Ma and rhyolites - 97 ± 5 Ma. Thus, we can assume an almost continuous stage of magmatic activity, which lasted in the interval 119 - 97 Ma ago and died out at the very beginning of the Late Cretaceous.

An analysis of the geological, petrochemical, and geochemical characteristics of these rocks suggests that they formed as intraplate formations and accompanied the final completion of the formation of the Mongol-Okhotsk orogen [8].

III stage. Magmatic formations, which replaced the rocks of the bimodal series, began to form 94 Ma. Since that time, intraplate formations of the riftogenic complex have been developing: trachyandesites-absarokites [26]. Trachiande-

sites belong to the potassium-sodium series (Na_2O/K_2O = 1.66 - 2.05), and absarokites (Na_2O/K_2O = 0.47) belong to potassium series; the amount of alkali varies from 6.35 to 9.01 wt%. Volcanites are characterized by low-moderate contents of MgO, TiO_2, with an Al_2O_3 content of 15.24 - 17.45 wt% (saturation index Al = 1.1 - 1.3).

The rocks are characterized by a differentiated REE spectrum (**Figure 5(a)**), with (La/Yb)n = 13.95 - 20.67. Europium anomaly is practically absent or reveals a weak positive anomaly: (Eu/Eu*)n = 0.79 - 1.03. They are characterized by moderate enrichment Ba (670 - 1540 ppm), Sr (440 - 950 ppm), K (14,600 - 28,400 ppm), Th (6.4 - 21.4 ppm), Rb (60 - 240 ppm) with elevated contents of Nb (до 22 ppm), Ta (1.68 ppm), Zr (330 ppm), Hf (10.4 ppm), Y (22.4 ppm), Yb (2.04 ppm) (**Figure 5(b)**).

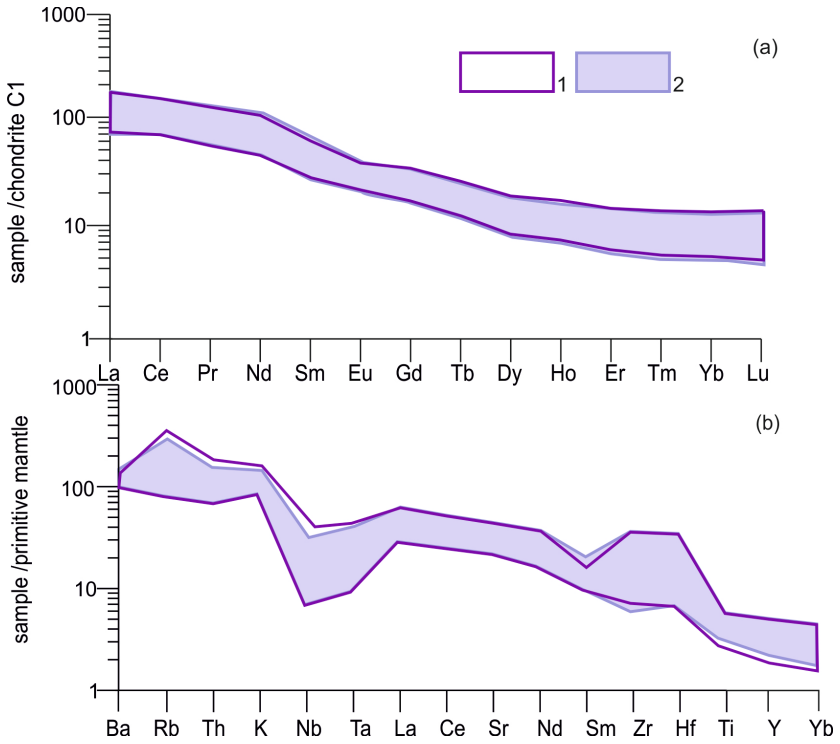

Figure 5. Concentrations of the rare elements of the rock intraplate series (94 - 88 Ma) standardized to the composition of Chondrite (a) and primitive mantel (b). Compositions of chondrite C_1 and primitive mantel are brought according to the data [19]. Northern frames (1) and Southern frames (2) EFMOOB.

Trachiandesites-absarokites are developed within the rift depressions in the northern and southern frames of the belt. They indicate the beginning of the destructive processes in the region.

4. Discussion

The analysis of the manifestation of Late Mesozoic magmatic activity in the frame of the eastern flank of the MOOB showed that synchronous geodynamic processes which were accompanied by the formation of magmatic complexes of

the same age and material composition took place in the region during Late Jurassic - Late Cretaceous.

1) Along the southern border of the MOOB, the Argun and Bureya-Jiamusi super terrains stand out, separated by the South Mongol-Khingan terrain (**Figure 1(b)**). The area distribution of all the above formations along the southern frame of the EFMOOB is cut off in the east by the structure of the Bureya-Jiamusi super terrains (**Figure 1(b)**). Within its limits, Late Mesozoic magmatites are asynchronous in time of formation of the rocks of the above complexes [3] [9]. Late Mesozoic magmatites within it are asynchronous in time of formation to the above-described rock complexes in the frame of the belt.

According to our data [3] [9], the Bureya-Jiamusi super terrain did not participate in the closure of the Mongol-Okhotsk basin. It is an independent structure that joined the Eurasian continent after the described geological events.

The distribution of the above-described rocks is cut off by the SSS structure in the west along the northern margin of the belt. Within this structure, magmatites known as the Selenga-Vitim volcano plutonic belt (SVVPB) [27] are widely developed.

A clear difference from the considered formations is established by the belt formation time, by the material composition of the composing magmatites. The rocks of calc-alkaline and bimodal volcano-plutonic series were formed in its early development stages ($C_2 - P_2$). The magmatites of the bimodal series were formed at the later stage (T) [27]. There are no analogues to these formations in the northern and southern frames of the MOOB. According to the data [12] [13], the northern boundary between the SSS and the DSS (**Figure 6(a)**) is represented by the Dzheltulak fault zone of the crustal bed. Within this zone, milonites, blastomilonites, blastocataclazites, sections of layer-by-layer schismation of rocks, and silicon-alkaline metasomatism are widely developed. The age of zircons from blastomilonites determined by the U-Pb method showed that there are formations of different ages: 1960 - 1930, 1750 - 1700, 1600 - 1500 Ma (determination by zircons), 2000 - 1350 Ma (by pyrochlore) [28]. Late Jurassic – Early Late Cretaceous volcanoplutonic complexes are widely manifested to the north-east of the Dzheltulak fault (**Figure 6(a)**). These formations are traceable to the east along the northern margin of the MOOB. These rocks are an analogue of the formations developed along the southern margin of the eastern flank belt [17] [23].

2) The eastern flank of the SSS borders with MOOB (**Figure 1(b)**) in the south through the North Tukuringra fault. A tectonic zone with a length of 800 km and a width of up to 50 km is distinguished along this boundary. This zone is composed with sedimentary and volcanogenic rocks metamorphosed in the amphibolite facies. Geochronological data defined by U-Pb method and isotope geochemical (Sm – Nd) studies of zone rocks [11] indicate the presence of metavolcanic rocks with an age of 193 ± 1 Ma; granitoids with an age of 370 Ma, which are characterized by minimal tNd (DM) = 1.1 BA. According to the values of tNd (DM), metamorphic rocks of the stratum decompose into two groups

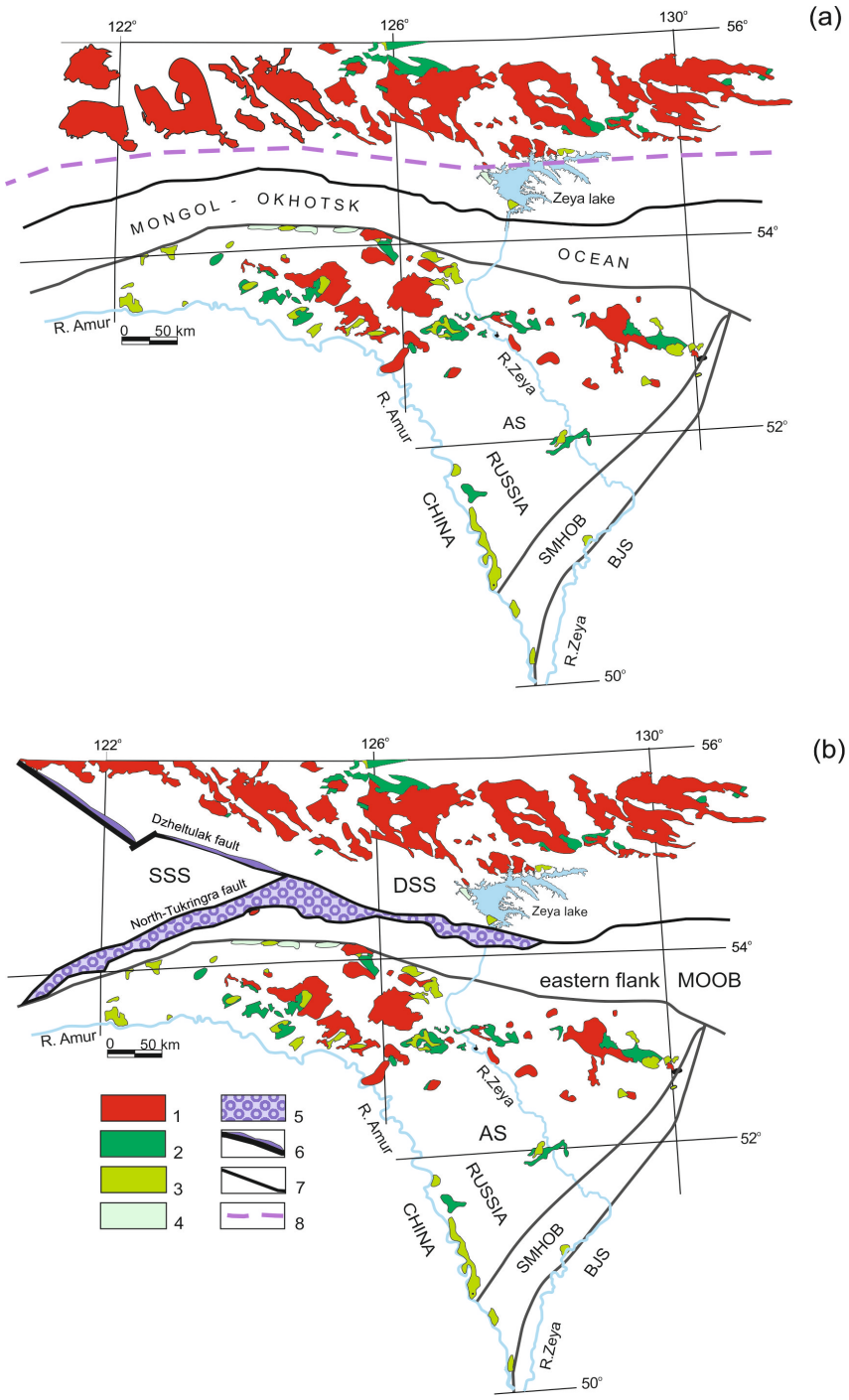

Figure 6. Scheme of the Late Mesozoic tectonic structure of the eastern flank of the MOOB and the location of magmatic formations in its frame: before the Cenozoic tectonic rearrangement (6 a) and after the Cenozoic tectonic rearrangement (6 b) according to [29]. Magmatites (1 - 3): 1—adakitic and calc-alkaline granitoids (145 - 126 Ma); 2—calc-alkaline volcanics (130 - 122 Ma); 3—magmatites of the bimodal series (119 - 97 Ma); 4—trachyandesites, absarokites of rifting (94 - 88 Ma); 5—Melange zone (according to [11]); 6—Dzheltulak fault zone; 7—Structure-forming tectonic boundaries; 8—Boundary of distribution of Late Mesozoic igneous complexes before tectonic rearrangement in the Cenozoic. Abbreviations are not indicated in the text: Bureya-Jiamusi superterrane (BJS), Argun Superterrane (AS); South Mongol-Khingan Orogenic Belt (SMKOB).

with tNd (DM) = 1.1 - 1.9 and tNd (DM) = 2.5 - 3.1 Ga. The authors [11] note that a clear spatial distribution of formations with Late Archean and Proterozoic tNd (DM) values is not detected. All these data allowed the authors to draw the following conclusions [11]: a) rocks of different ages are combined within the zone; b) the zone is a tectonic melange composed of metamorphosed rocks of the Mesozoic, Paleozoic and Early Precambrian ages; c) the formation of the zone occurred in the Mesozoic, during the Late Jurassic - Early Cretaceous collision processes. The latter fact is refuted by the authors themselves [11]: findings of Mesozoic rocks within the zone. This indicates that the formation of the melange zone occurred much later.

3) Magmatic processes in the northern and southern rims of the MOOB occurred simultaneously and were associated with the closure of the Mongolian-Okhotsk basin. What was provoked by the convergence of the Siberian and North China cratons. This process was accompanied by synchronous subduction of the Mongolian-Okhotsk basin in both northern and southern directions. Therefore, it is reasonable to assume that by the end of the Late Mesozoic, all the described magmatites were located at an equal distance from the supposed subduction boundaries. This regularity was most clearly preserved in the northern frame of the MOOB (**Figure 6(a)**). In this case, the position of the CCC did not correspond to its current state at that time. Most likely, SSS "wedged" between the MOOB and the southern margin of the Siberian craton after the end of the Late Mesozoic magmatism, later than 88 Ma (**Figure 6(b)**).

According to the geophysics data, the heterogeneous layering of the lithosphere structure is established at the base of the SSS, which is a sign of horizontal movements in the earth's crust and in the subcrustal space. It was found [12] [13] [14] that within the zone there are deep inclined interfaces between both modern and earlier foundations. The modern (Late Cenozoic) borders have a southern fall, and the paleo-borders have the northern one. Probably, the paleo-boundaries of the northern occurrence arose as a result of the Late Mesozoic subduction processes, when the oceanic bed of the Mongol-Okhotsk basin subducted under the continental margin of the southern margin of the Siberian craton. Late Cenozoic borders indicate the existence of tectonic rearrangements in this period of time.

Such global tectonic transformations could only be associated with global tectonic rearrangements in neighboring, interdependent territories. Such transformations include tectonic events occurring during the collision of the Indian Plate and the Eurasian continent in the Cenozoic. There are various assumptions about the age of this process. Some consider 65 Ma the most likely age [30] [31], others 45 - 55 Ma [32] [33] or 35 Ma [34]. But most researchers attribute these processes to the 55 - 50 Ma period [35] [36] [37]. These authors of the researches [38] [39] [40] [41] reached the same conclusion. They believe that initially the Indian plate was subducted under the Eurasian continent. This led to the formation of an accretionary prism. But in about 25 - 20 Ma, a continent-continent collision began, which led to the extrusion of the Great Himalayas along southern Tibet and to the beginning of the deformation of more remote territories in

Central Asia: the deformation and the rise of the Tien Shan [42]. This conclusion agrees with the age of post-collisional magmatism in Southern Tibet, which began 26 Ma ago [43] [44].

According to [45], the collision influence zone of the of the Indian Plate and Eurasia consists of six tectonic domains, among which there is a Central Asian domain with a deformation region extending from the Tien Shan in the south to the Baikal rift zone in the north. The formation of a mountainous terrain in the Tien Shan was completed in the Pliocene (review in work [46]). The duration of the orogenesis stage is almost 15 Ma and corresponds to the interval of 25 - 10 Ma. Based on these considerations, it can be stated that the post-Mesozoic tectonic restructuring in the north-western frame of the MOOB occurred at the Oligocene—Miocene border. It was during this period, under the influence of the processes occurring between the Indian plate and the Eurasian continent, when the Indian plate moved in a northeast direction at an angle close to 20 degrees, the SSS was displaced and wedged between the MOOB and the southern frame of the Siberian craton—DSS. It can be assumed that the entire north-western frame of the MOOB was affected by this process. This conclusion has indirect evidences. Symmetrically located magmatic complexes of the Paleozoic - Early Mesozoic are developed in the frame of the western flank of the MOOB (**Figure 7**). The scheme clearly establishes the displacement of these complexes along the north-west framing of the belt relative to their location in the south-east framing.

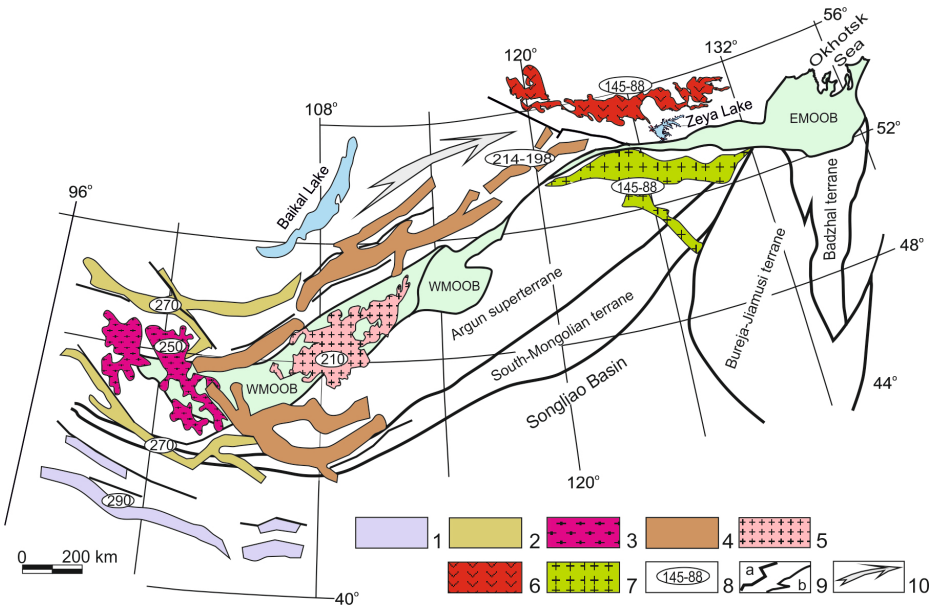

Figure 7. Scheme of the magmatic complexes of the Late Paleozoic-Mesozoic framed by MOOB. The scheme is made using the data by [29] [47]. The area of distribution of magmatic associations: Late Carboniferous - Early Permian bimodal series and granitoids (1), Permian bimodal series (2) and granitoids (3), Early Mesozoic bimodal series (4) and granitoids (5), Late Mesozoic volcano plutonic complexes with a predominance of plutonic rocks (6) and with a predominance of volcanogenic rocks (7), Age of rocks in Ma (8), Tectonic faults (9): structural (a), others (b), The intended direction of movement of the SSS (10).

5. Conclusions

Magmatic activity in the frame of the eastern flank of the MOOB ended at the beginning of the Late Cretaceous—no later than the Santonian. In fact, since that time, the territory has been in a state of rest: the formation of platform formations begins [48]. And this process continues to this day. But it was during this period that the tectonic restructuring of the region took place. It was not accompanied by any magmatic events. As a result of this restructuring, in the region of the 120th meridian, the SSS wedged itself between the southern framing of the Siberian Craton and MOOB. The belt was divided into two flanks: western and eastern.

What could be the "driving force" of global movements of such large geological objects? It has been established that the Central Asian region, extending from the Tien Shan in the south to the Baikal rift zone in the north, is a zone of influence of the collision of the Indian Plate and the Eurasian continent [45]. Hence it follows that the junction of the MOOB structures and the southern framing of the Siberian Platform in the Cenozoic was under the influence of distant collisional processes. Since the structures described are interdependent, this should have influenced the evolution of MOOB. It can be assumed that the "driving force" of the SSS movement was the collisional processes occurring between the Indian and Eurasian plates at the boundary of the Oligocene and Miocene. It is these processes that changed the contour of the MOOB in the post-Mesozoic time.

Acknowledgements

The author is grateful to the staff of the IGiP FEB RAS (Blagoveschensk, Amur region, Russia) Elena V. Ushakova; ITiG FEB RAS (Hbarovsk, Russia) Dmitry V. Avdeev, Anna V. Shtareva, Larisa S. Bokovenko, Anastasia Lushnikova and Valentina E. Zazulina; to the staff of IGEM RAS (Moscow, Russia) Andrey V. Chugaev and Tatyana I. Oleinikova for conducting out analytical studies of the rocks.

Conflicts of Interest

The author declares no conflicts of interest regarding the publication of this paper.

References

[1] Parfenov, L.M., Popeko, L.I. and Tomurtogoo, O. (1999) The Problems of Tectonics of the Mongol-Okhotsk Orogene. *Russian Journal of Pacific Geology*, **18**, 24-43.

[2] Bouysse, P. (2009) Geological Map of the World, 1:50 000000. Commission for the Geological Map of the World, Paris. http://www.ccgm.org/

[3] Derbeko, I. (2018) Bureya-Jiamusi Superterrane: Tectonic and Geodynamic Processes in Late Mesozoic-Cenozoic. In: Sharkov, E., Ed., *Tectonics*: *Problems of Regional Settings*, InTech Open, London, 33-45.

[4] Antonov, A.U. (2007) Geochemistry and Petrology of Mesozoic—Cainozoic Magmatic Formations of Southern Framing of Aldansky Shield. The Problems of Geo-

dynamics. *Russian Journal of Pacific Geology*, **26**, 56-81.

[5] Sorokin, A.A., Ponomarchuk, V.A., Sorokin, A.P. and Kozyrev. S.K. (2004) Geochronology and Correlation of Mesozoic Magmatic Formations of the Northern Edge of Amur Superterrain. *Stratigraphy and Geological Correlation*, **12**, 36-52.

[6] Strikha, V.E. (2006) Late Mesozoic Collisional Granitoids of Upper Priamurie: New Geochemical Data. *Geochemistry*, **8**, 855-872. https://doi.org/10.1134/S0016702906080040

[7] Derbeko, I. (2012) Bimodal Volcano-Plutonic Complexes in the Northern Frames of Eastern Section of Mongol-Okhotsk Orogenic Belt. *Journal of Earth Science and Engineering*, **2**, 84-96.

[8] Derbeko, I.M. (2012) Bimodal Volcano-Plutonic Complexes in the Frames of Eastern Member of Mongol-Okhotsk Orogenic Belt, as a Proof of the Time of Final Closure of Mongol-Okhotsk Basin. In: Stoppa, F., Ed., *Updates in Volcanology—A Comprehensive Approach to Volcanological Problems*, InTech Open, Rijeka, 99-124.

[9] Derbeko, I.M. (2013) The Role of the Andesitic Volcanism in the Understanding of Late Mesozoic Tectonic Events of Bureya-Jziamysi Superterrain, Russian Far East. In: Nemeth, K., Ed., *Updates in Volcanology—New Advances in Understanding Volcanic Systems*, InTech Open, New Zealand, 91-115. https://doi.org/10.5772/51908

[10] Derbeko, I.M. and Chugaev, A.V. (2020) Late Mesozoic Adakite Granites of the Southern Frame of the Eastern Flank of the Mongol-Okhotsk Orogenic Belt: Material Composition and Geodynamic Conditions of Formation. *Geodynamics & Tectonophysics*, **11**, 474-490. https://doi.org/10.5800/GT-2020-11-3-0487

[11] Velikoslavinsky, S.D., Kotov, A.B., Salnikova, E.B., Larin, A.A., *et al.* (2012) On the Age of the Ustygilyuya Stratum of the Mill Selenga-Stanovoy Superterrane Complex of the Central Asian Fold Belt. *Doklady Earth Sciences*, **444**, 402-406.

[12] Didenko, A.N., Efimov, A.S., Nelyubov, P.A., *et al.* (2013) Structure and Evolution of the Earth's Crust in the Region of Junction of the Central Asian Fold Belt and the Siberian Platform: Skovorodino-Tommot Profile. *Russian Geology and Geophysics*, **54**, 1236-1249. https://doi.org/10.1016/j.rgg.2013.09.008

[13] Didenko, A.N., Kaplun, V.B., Malyshev, Y.F. and Shevchenko, B.F. (2010) Lithospheric Structure and Mesozoic Geodynamics of the Eastern Central Asian Orogen. *Russian Geology and Geophysics*, **51**, 492-506. https://doi.org/10.1016/j.rgg.2010.04.006

[14] Shevchenko, B.F., Popeko, L.I. and Didenko, A.N. (2014) Tectonics and Volution of the Lithosphere of the Eastern Fragment of the Mongol-Okhotsk Orogenic Belt. *Geodynamics & Tectonophysics*, **5**, 667-682. https://doi.org/10.5800/GT-2014-5-3-0148

[15] Kheraskova, T.N., Yakovlev, D.V., Pimanova, N.N. and Berezner, O.S. (2018) Conjugation with the Central Asian Foldbelt: Interpretation of the 3DV and Tynda-Amurzet Transects. *Geotectonics*, **52**, 1-21. https://doi.org/10.1134/S0016852118010089

[16] Derbeko, I.M. (2016) Adakite Magmatism as an Indicator of the Beginning of the Subduction Regime along the Southern Border of the Eastern Link of the Mongolo-Okhotsk Orogenic Belt. Geological Processes in the Lithospheric Plate's Subduction, Collision, and Slide Environments. In: Khanchuk, A.I., Ed., *Proceedings of Third Russian Conference with Foreign Participants*, Dalnauka, Vladivostok, 268-271.

[17] Derbeko, I.M. (2018) Magmatism as an Indicator of Synchronous Geodynamic

Events in the Frame of the Mongol-Okhotsk Orogenic Belt. In: Degtyarev, K.E., Ed., *Lth Tectonic Proceedings of the Meeting*, GEOS, Moscow, 142-146.

[18] Zen, E.A. (1986) Aluminum Enrichment in Silicate Melts by Fractional Crustallization: Some Mineralogic and Petrographic Constraints. *Journal of Petrology*, **27**, 1095-1117. https://doi.org/10.1093/petrology/27.5.1095

[19] Sun, S.S. and McDonough, W.F. (1989) Chemical and Isotopic Systematics of Oceanic Basalts: Implications for Mantle Composition and Processes. *Geological Society*, *London*, *Special Publications*, **42**, 313-345. https://doi.org/10.1144/GSL.SP.1989.042.01.19

[20] Martin, H. (1993) The Mechanisms of Petrogenesis of the Archaean Continental crust—Comparison with Modern Processes. *Lithos*, **46**, 373-388. https://doi.org/10.1016/0024-4937(93)90046-F

[21] Martin, H. (1999) Adakitic Magmas: Modern Analogues of Archaean Granitoids. *Lithos*, **46**, 411-429. https://doi.org/10.1016/S0024-4937(98)00076-0

[22] Defant, M.J., Jackson, T.E., Drummond, M.S., Bellon, H., Feigenson, M.D., Maury, R.C. and Stewart, R.H. (1992) The Geochemistry of Young Volcanism throughout Western Panama and South-Eastern Costa Rica: An Overview. *Journal of the Geological Society*, **149**, 569-579. https://doi.org/10.1144/gsjgs.149.4.0569

[23] Derbeko, I.M. (2007) Late Mesozoic Geodynamical Formation on the Territory of the Eastern edge of Mongol-Okhotsk Orogenic Belt (Russia). Tectonics and Metallogeny of the Circum-North Pacific and Eastern Asia. In: Didenko, A.N., Ed., *Proceedings of the Leonid Parfenov Memorial Conference*, IT and FEB RAS, Khabarovsk, 146-149.

[24] Kozyrev, S.K., Volkova, Y.R. and Ignatenko, N.N. (2016) State Map of the Russian Federation-Scale 1: 200 000. 2nd Edition, Series Zeya, Sheet N-51-XXIV, Explanatory Note, Moscow Branch of FSBI "VSEGEI", Moscow.

[25] Kozyrev, S.K., Volkova, Y.R. and Ignatenko, N.N. (2016) State map of the Russian Federation-scale 1: 200 000. 2nd Edition, Series Zeya, Sheet N-51-XXIII, Explanatory Note, Moscow Branch of FSBI "VSEGEI", Moscow.

[26] Derbeko, I.M. and Markevich, V.S. (2013) Late Mezozoic Subalkai Volcanism of the South Framing of the Eastern Link of Mongol-Okhotsk Orogenic Belt. *Natural and Technical Sciences*, **2**, 135-143.

[27] Gordienko, I.V. and Kuzmin, M.I. (1999) Geodynamics and Metallogeny of the Mongol-Transbaikalian Region. *Russian Geology and Geophysics*, **40**, 1545-1562.

[28] Arkhangelskaya, V.V., Kazansky, V.I., Prokhorov, K.V. and Sobachenko, V.N. (1993) Geological Structure, Zoning and Formation Conditions of the Katuginsky Ta-Nb-Zr Deposit. *Russian Geology and Geophysics*, **54**, 115-131.

[29] Geological Map of Amur Region and Adjacent Scale 1:2500000 (1996) Harbin—Sankt-Petersburg—Blagoveshchensk: Roskomnedra, VSEGEI, MG&MR of China.

[30] Ding, L., Kapp, P. and Wan, X. (2005) Paleocene-Eocene Record of Ophiolite Obduction and Initial India-Asia Collision, South Central Tibet. *Tectonics*, **24**, TC3001. https://doi.org/10.1029/2004TC001729

[31] Cai, F., Ding, L. and Yue, Y. (2011) Provenance Analysis of Upper Cretaceous Strata in the Tethys Himalaya, Southern Tibet: Implications for Timing of India-Asia Collision. *Earth and Planetary Science Letters*, **305**, 195-206. https://doi.org/10.1016/j.epsl.2011.02.055

[32] Dupont-Nivet, G., Lippert, P.C., Hinsbergen, D.J., Meijers, M.J and Kapp, P. (2010) Palaeolatitude and Age of the Indo-Asia Collision: Palaeomagnetic Constraints. *Geophysical Journal International*, **182**, 1189-1198.

https://doi.org/10.1111/j.1365-246X.2010.04697.x

[33] Molnar, P. and Tapponnier, P. (1975) Cenozoic Tectonics of Asia: Effects of a Continental Collision. *Science*, **189**, 419-426. https://doi.org/10.1126/science.189.4201.419

[34] Aitchison, J.C., Ali, J.R. and Davis, A.M. (2007) When and Where Did India and Asia Collide? *Journal of Geophysical Research*: *Solid Earth*, **112**, B05423. https://doi.org/10.1029/2006JB004706

[35] Zhu, B., Kidd, W.S.F., Rowley, D.B., Currie, B.S. and Shafique, N. (2005) Age of Initiation of the India-Asia Collision in the East-Central Himalaya. *The Journal of Geology*, **113**, 265-285. https://doi.org/10.1086/428805

[36] Green, O.R., Searle, M.P., Corfield, R.I. and Corfield, R.M. (2008) Cretaceous-Tertiary Carbonate Platform Evolution and the Age of the India-Asia Collision along the Ladakh Himalaya (Northwest India). *The Journal of Geology*, **116**, 331-353. https://doi.org/10.1086/588831

[37] Najman, Y., Appel, E., Boudagher-Fadel, M. *et al.* (2010) Timing of India-Asia Collision: Geological, Biostratigraphic, and Palaeomagnetic Constraints. *Journal of Geophysical Research*: *Solid Earth*, **115**, B12416. https://doi.org/10.1029/2010JB007673

[38] O'Neill, C., Muller, D. and Steinberger, B. (2005) On the Uncertainties in Hot Spot Reconstructions and the Significance of Moving Hot Spot Reference Frames. *Geochemistry*, *Geophysics*, *Geosystems*, **6**, Q04003. https://doi.org/10.1029/2004GC000784

[39] Van Hinsbergen, D.J.J., Kapp, P., Dupont-Nivet, G., Lippert, P.C., DeCelles, P.G. and Torsvik, T.H. (2011) Restoration of Cenozoic Deformation in Asia and the Size of Greater India. *Tectonics*, **30**, TC5003. https://doi.org/10.1029/2011TC002908

[40] Van Hinsbergen, D.J.J., Steinberger, B., Doubrovine, P.V. and Gassmöller, R. (2011) Acceleration and Deceleration of India-Asia Convergence since the Cretaceous: Roles of Mantle Plumes and Continental Collision, *Journal of Geophysical Research*: *Solid Earth*, **116**, B06101. https://doi.org/10.1029/2010JB008051

[41] Van Hinsbergen, D.J.J., Lippert, P.C., Dupont-Nivet, G., McQuarrie, N., Doubrovine, P.V., Spakman, W. and Torsvik, T.H. (2012) Greater India Basin Hypothesis and a Two-Stage Cenozoic Collision between India and Asia. *Proceedings of the National Academy of Sciences of the United States of America*, **109**, 7659-7664. https://doi.org/10.1073/pnas.1117262109

[42] Sobel, E.R., Chen, J. and Heermance, R.V. (2006) Late Oligocene—Early Miocene Initiation of Shortening in the Southwestern Chinese Tian Shan: Implications for Neogene Shortening Rate Variations. *Earth and Planetary Science Letters*, **247**, 70-81. https://doi.org/10.1016/j.epsl.2006.03.048

[43] Xia, L., Li, X., Ma, Z., Xu, X. and Xia, Z. (2011) Cenozoic Volcanism and Tectonic Evolution of the Tibetan Plateau. *Gondwana Research*, **19**, 850-866. https://doi.org/10.1016/j.gr.2010.09.005

[44] Zhao, Z., Mo, X., Dilek, Y., Niu, Y., DePaolo, D.J., Robinson, P., Zhu, D., Sun, C., Dong, G., Zhou, S., Lui, Z. and Hou, Z. (2009) Geochemical and Sr-Nd-Pb-O Isotopic Compositions of the Post-Collisional Ultrapotassic Magmatism in SW Tibet: Petrogenesis and Implications for India Intracontinental Subduction beneath Southern Tibet. *Lithos*, **113**, 190-212. https://doi.org/10.1016/j.lithos.2009.02.004

[45] Yin, A. (2010) Cenozoic Tectonic Evolution of Asia: A Preliminary Synthesis. *Tectonophysics*, **488**, 293-325. https://doi.org/10.1016/j.tecto.2009.06.002

[46] Burtman, V.S. (2012) Geodynamics of Tibet, Tarim and Tien-Shan in the Late Ce-

nozoic. *Geotectonics*, **3**, 18-46. https://doi.org/10.1134/S0016852112030028

[47] Bogatikov, O.A. and Kovalenko, V.I. (2006) Types of Magma and Their Sources in the History of the Earth. Part 2. Rare-Earth Magmatism: Association of the Rocks, Their Content and Sources of Magmas, Geodynamical Situations of the Formation. Institute of Geology of ore Deposits Russian Academy of Science, Moscow.

[48] Sorokin, A.P. (2013) Young Platforms of the Eastern Margin of Euroasia (Deep Structure, Formational Condition and Metallogeny). Dalnauka, Vladivostok.